JOURNAL OF AIRCRAFT
Vol. 43, No. 2, March–April 2006

Active Flutter Control with V-Stack Piezoelectric Flap Actuator

Emil V. Ardelean*
Science Applications International Corporation, Albuquerque, New Mexico 87106
Mark A. McEver†
L-3 Communications Corporation, Pittsburgh, Pennsylvania 15238
and
Daniel G. Cole‡ and Robert L. Clark§
Duke University, Durham, North Carolina 27708

Aeroelastic control of wings using distributed, trailing-edge control surfaces is of interest for maneuvers, gust alleviation, and flutter suppression. The use of high-energy-density, piezoelectric materials as motors provides an appealing solution to the problem of flutter suppression. A new piezoelectric actuator, the V-stack piezoelectric actuator, was designed and bench tested at Duke University. This actuator meets the requirements for trailing-edge flap actuation in both stroke and force. It is compact, simple, and sturdy and leverages stroke geometrically with minimum force penalties while displaying linearity over a wide range of stroke. Integration of the actuator inside a structure requires minimal modifications. The shape of the actuator makes it extremely suitable for trailing-edge flap actuation, eliminating the need for a push rod. A typical section prototype was constructed and tested experimentally in the wind tunnel at Duke University. This experiment was designed for preliminary evaluation of the actuation concept. During bench tests the desired flap deflection of ±5 deg was obtained. Wind-tunnel experiments showed that air flow has little influence on flap deflection, suggesting good actuation authority. Actuator-flap frequency bandwidth achievable for this experiment, in the context of ±5 deg flap deflection, was sufficient and facilitated control design. Positive position feedback (PPF) control was used to add damping to the unstable flutter mode. Operating in closed loop, the flutter was suppressed at the speed at which the flutter occurred open loop, and the flutter speed was increased by more than 30%.

Nomenclature

a	=	position of the elastic axis with regard to midchord point in fractions of the semichord
b	=	semichord
c	=	position of the hinge line with regard to midchord point in fractions of the semichord
I_{CG}	=	moment of inertia of the wing model with regard to its center of mass
I_{fCG}	=	moment of inertia of the flap with regard to its center of mass
I_{wCG}	=	moment of inertia of the wing model without flap with regard to its center of mass
K_h	=	plunge stiffness
K_α	=	pitch stiffness
K_β	=	flap stiffness
m	=	total mass of the wing model
m_{bl}	=	mass of the lower mounting block
m_{bu}	=	mass of the upper mounting block (including the sensor)
m_f	=	mass of the flap
s	=	actuator stroke
U_∞	=	airflow speed
x_{CG}	=	position of the center of mass of the wing (including flap) with regard to the elastic axis
x_{CGf}	=	position of the center of mass of the flap with respect to hinge line
x_{CGw}	=	position of the center of mass of the wing without flap with regard to the elastic axis

Received 13 July 2004; revision received 12 May 2005; accepted for publication 17 May 2005.

*Senior Mechanical Engineer, 2109 Air Park Road. Member AIAA.
†Control Systems Engineer, 615 Epsilon Drive. Member AIAA.
‡Senior Research Scientist, Pratt School of Engineering, Mechanical Engineering and Materials Science Department. Member AIAA.
§Thomas Lord Professor of Engineering, Pratt School of Engineering, Mechanical Engineering and Materials Science Department. Member AIAA.

Introduction

IN real-life applications aerolastic control is done using discrete control surfaces because of practical aspects (thus are easy to manufacture, actuate, and maintain). Discrete trailing-edge control surfaces (flaps and ailerons) are widely used for aeroelastic control because of simplicity, inherent stability, and effectiveness of the solutions. Various solutions exist for trailing-edge flap actuation; however, flutter alleviation requires actuation systems capable of producing large force and large stroke (up to ±6 deg flap deflection) over a wide frequency range (up to 25–30 Hz). Conventional hydraulic systems, widely used for actuation of conventional aeroelastic control systems, are relatively slow (limited bandwidth) and complicated.

Recent developments of new piezoceramic actuation systems have made flutter alleviation using trailing-edge flaps more feasible for small aircraft such as unmanned aerial vehicles (UAVs). The latest results are encouraging in spite of the fact that the piezoelectric transducers are not well developed for large stroke applications; they are used in numerous other applications.[1–6]

At Duke University, as part of an effort to build an adaptive high-aspect-ratio wing, a new actuator, called V-stack piezoelectric actuator, was developed.[6] Preliminary tests performed on the actuator indicated that integration of the actuator into a wing model for driving a trailing-edge flap should give good results.[7] The actuator uses two stacks of high-performance piezoceramic as active elements. The stacks are symmetrically positioned with respect to a central element (lever) and work complementarily. The shape of the actuator facilitates its integration into an airfoil, requiring very few additional elements. This helps to make the structure simple and efficient (mass, stiffness, construction, etc.).

A typical section (NACA 0015) suitable for testing in the wind tunnel at Duke University, referred to as the wing model in the

following, was constructed and tested. The primary objective of the experiment was to increase the flutter boundary by controlling the flap in a closed-loop fashion. Aeroelastic analysis of the wing predicted the flutter free stream velocity of 19 m/s and a flutter frequency of 4.2 Hz. The wing was first tested on the bench and then tuned for testing in the wind tunnel. The tuning was related primarily to the actuator-flap system because of issues addressed in the following sections.

Experimental Model

The shape of the actuator (V) triggered the idea that the actuator could be mounted in the direction of the chord. In this case, the actuator plane would be perpendicular to the wing plane and the direction of the actuator output would be also perpendicular to the wing plane. By positioning the actuator chordwise, the output point could be located very close to the hinge of the flap, eliminating the need for a push rod. Without a push rod, the actuation mechanism can be simpler, lighter, and stiffer. Also, the internal structure of a particular wing would be minimally disturbed. A design analysis revealed that a crank-slider-like mechanism would be a better solution than a floating link. As a result, the design of the actuator tip was modified to accommodate a slider.

Figure 1 presents a cross-sectional view of the design of the actuator integration into a wing model. The actuator, 3, is attached to the ribs, 1, through the support, 2, designed such that it will mount on existing elements of the structure. Two bolts are used to secure the actuator in place. For sophisticated constructions, one would use an adjustable support to tune the desired position of the actuator (chordwise and spanwise). However, for the purpose of this work a careful machining of the parts was preferred.

The necessary torque for flap actuation is realized by applying the actuator output force at an offset distance, r_β, from the flap hinge. Upon applying voltage to the actuator piezoelectric stacks, the tip of the actuator moves up and down and pushes the slider (mounted on a pin), causing the flap to rotate about the hinge line, 5. There is a very low-clearance fit between the actuator tip and the slider to avoid undesirable nonlinearities (free play) and, at the same time, to allow free motion of the slider along the slot. The motion of the slider along the slot is required to compensate for the change in distance between the pivot point of the lever and the axis of the flap-actuation pin during operation. To minimize friction between the slider and the actuator tip, the slider is made of bronze and the actuator tip is made of high-strength steel. The slider is mounted (tight fit) on a pin that is supported on two ball bearings mounted in a support, 6. The flap is mounted on ball bearings for minimal friction losses.

The support, 6, can slide along a slot machined in the flap rib, 7, and this permits tuning of the actuator-flap system: flap deflection and flap bandwidth. A trade-off between the two exists because for large flap deflection one would obtain smaller bandwidth and vice versa. Tuning is realized by adjusting the distance, r_β, between the flap hinge and slider pivot axis.

The typical section model was designed and constructed to fit in Duke's low-speed wind tunnel, using a testing rig used by other Duke researchers for aeroelastic experiments on typical sections.[8–11] The geometric, inertia, and stiffness parameters for the test section are given in Table 1. The rig consists of two almost-identical assemblies (mechanisms), mounted above and below the testing section of the wind tunnel. The schematic of the mechanisms is presented in Fig. 2. The typical section is mounted on two bearings (top and bottom) using two short shafts that fit in the aluminum tube at quarter chord. The bearings allow the shafts to rotate freely, thus permitting pitch degree of freedom. The housings of the bearings are fixed on moving support plates that are further supported, each on two leaf springs. The leaf springs are clamped in the fixed support block and allow plunge degree of freedom and provide plunge stiffness at the same time. Pitch stiffness is provided by a steel wire subjected to bending (upper support only). The wire runs through a hole drilled in the upper mounting shaft and is pinned at both ends on the moving support plate. Stiffness in both plunge and pitch can be adjusted by adjusting the length of the leaf springs and distance between support points of the steel wire respectively. Angular displacement sensors (Lucas Shaevitz) are used to directly measure displacement for pitch and flap and indirectly for plunge. The testing rig brings additional mass into the system to be tested in the wind tunnel. The added mass is significant only for plunge motion and does not affect pitch-support plates, only translate, as shown in Fig. 2.

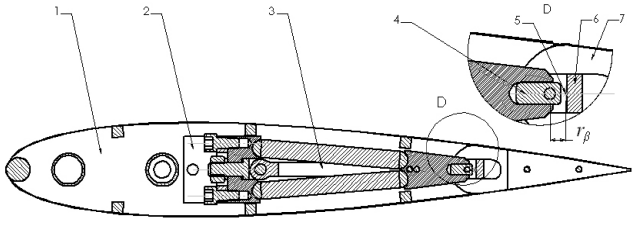

Fig. 1 Actuator integration into the wing (SolidWorks model): 1, rib; 2, actuator support; 3, actuator; 4, slider; 5, hinge line; 6, ball-bearing support; and 7, flap rib.

Table 1 Parameters of the typical section model and testing rig

Parameter	Unit	Value
	Dimensions	
Span	m	0.525
Chord	m	0.360
b	m	0.180
a	——	−0.5
c	——	0.5
	Inertial characteristics	
m	kg	2.610
m_w	kg	2.258
m_f	kg	0.352
x_{CG}	m	0.050
x_{CGw}	m	0.026
x_{CGf}	m	0.025
I_{CG}	kg × m^2	2.439×10^{-2}
Iw_{CGw}	kg × m^2	1.5×10^{-2}
If_{CGf}	kg × m^2	2.694×10^{-4}
S_α	kg × m	0.1305
S_β	kg × m	0.0088
m_{bu}	kg	0.644
m_{bl}	kg	0.392
	Stiffness characteristics	
K_h	N/m	1055.12
K_α	Nm/rad	32.28
K_β	Nm/rad	13.06

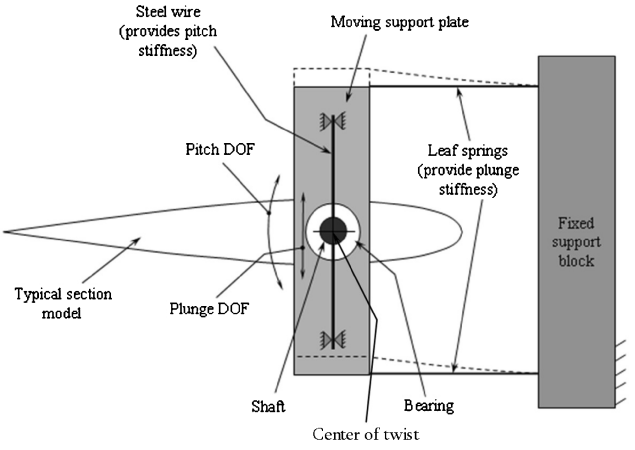

Fig. 2 Schematic of the testing rig.

Preliminary Tests

Preliminary tests were conducted to verify the experimental rig before the wind-tunnel experiments. During the design of the

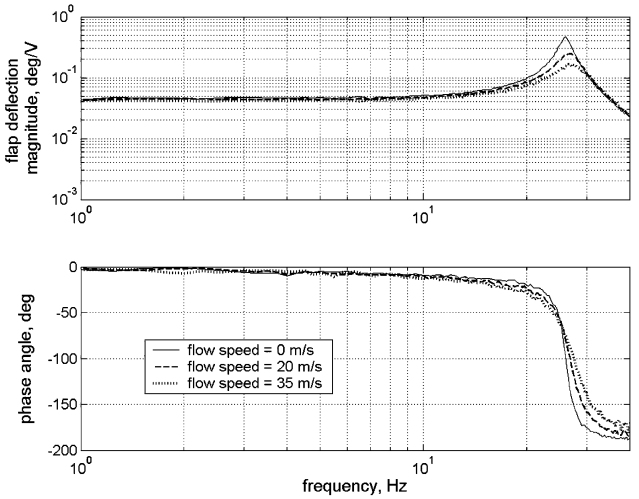

Fig. 3 Flap frequency response (uncoupled).

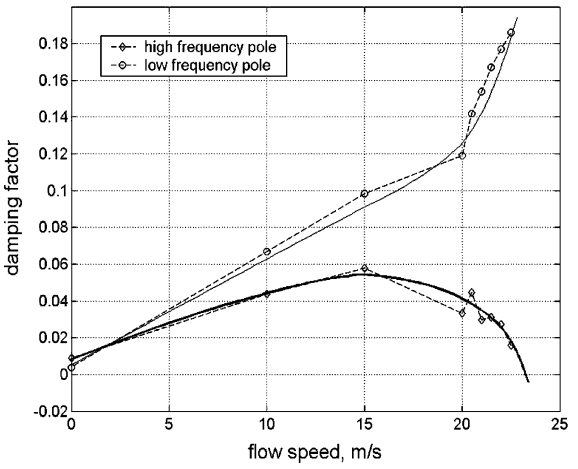

Fig. 4 Open-loop variation of the damping factor vs flow speed.

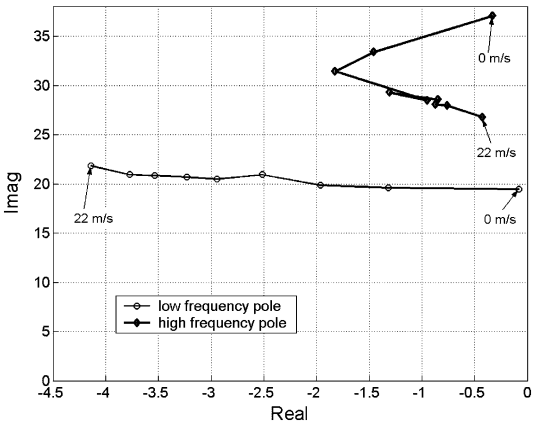

Fig. 5 Experimental pole migration for open-loop aeroelastic system.

experimental model two main objectives were targeted, namely, quasi-static angular deflection of the flap in excess of ±5 deg and bandwidth of the actuator-flap system exceeding natural frequencies in pitch and plunge. A large angle of deflection gives good control authority and a large bandwidth of the actuator-flap system will facilitate control design because the dynamics of the actuator flap will not influence the aeroelastic system dynamics.

Figure 3 presents the frequency response of the actuator-flap system in the absence of flow along with frequency responses obtained for flow speeds of 20 and 35 m/s. Observe that, regardless of the flow speed, flap response is flat up to about 10 Hz. Also observe that as the flow speed increases more damping is added to the system.

To analyze the fully coupled dynamic of the aeroelastic system in the absence of flow, the wing model was placed in the wind tunnel in the position it would be eventually tested under flow conditions, and all three degrees of freedom were allowed. The excitation of all three degrees of freedom was provided by exciting the flap with 100-Hz white noise. Resonant frequencies were found at 3.1, 5.9, 9, and 31 Hz. Because the connection between the upper and lower mounting blocks was not perfectly rigid, a plunge natural mode at 9 Hz is present.

Open-Loop Characteristics

The main objective for open-loop experiments was to determine flow speed and frequency at flutter. To this end, frequency-domain system identification of the aeroelastic system was performed for flow speeds from zero to a value close to the flutter speed. For $U_\infty < 10$ m/s, the reference flap motion was commanded using a white-noise excitation signal. However, for $U_\infty \geq 10$ m/s, the ambient wind-tunnel "noise" was significant compared to the motion generated by white noise to the flap. To obtain a satisfactory signal-to-noise ratio above 10 m/s, the frequency response was measured using a swept-sine analysis. Frequency responses from commanded flap deflection to pitch and plunge displacements were estimated by commanding a sinusoidal flap deflection of 2 deg. Continuous-time state-space models were then fit to estimated frequency responses using frequency-domain system-identification software. Parameters of interest, namely damping ratios and pole locations, were then obtained from these models.

Flutter speed U_F can be determined by representing the damping factor as a function of the flow speed. The speed for which the damping factor becomes zero is the flutter speed. Damping factors associated with the two poles of interest for different flow speeds can be found from the continuous-time models obtained as described previously. Figure 4 presents the variation of the damping factor with flow speed. Because system identification for an unstable system is not possible, U_F can be found by extrapolating experimental data. For this case it is $U_F \simeq 23$ m/s, which is ∼21% greater than the theoretical value. This difference is likely to be due to model simplicity because effects of the wind-tunnel walls, air temperature, and humidity were not taken into account.

Figure 5 presents migration of the two complex conjugate pairs of poles of interest for flow from 0 to 22 m/s. Note that the poles associated with pitch tend to become unstable, migrating toward the imaginary axis and eventually crossing into the right-hand-side plane, whereas damping of the plunge poles increases. The experimental flutter frequency is 4.3 Hz, accurately predicted by the aeroelastic model.

Control Design

The problem of flutter suppression is one of the most important objectives in aeroelastic control. The goal is stabilization of an unstable plant and delaying the onset of flutter until a higher speed. Instability occurs when damping associated with a pole of the aeroelastic system (a dynamic system in general) becomes negative; that is, the pole migrates into the right-hand plane. To prevent the pole from crossing into the right-hand plane, damping has to be added to the pole by using a suitable controller, therefore moving the pole into the stable region. By stabilizing an aeroelastic system that would otherwise encounter instability, the operational envelope of that system is increased.

Significant effort has been devoted to the subject of active flutter control using control strategies including classical, modern, LQR, LQG, robust $\mathcal{H}_\infty$, and $\mathcal{H}_2$ (see Refs. 5, 10–21). Although many researchers presented successful experimental demonstrations, in most cases performances are rather modest. Significant increase of the flutter speed (∼50%) for a rectangular HAR wing (AR = 10) was obtained by Borglund and Kuttenkeuler.[5] Using robust control design, Vipperman et al.[10] extended the flutter boundary of a typical section model by roughly 10%. Heeg[19] reported a 20% increase of flutter speed for an experimental model using piezoelectric actuation

and simple SISO feedback control. Cox[11] also reported a 20% increase of the flutter boundary of a typical section by successfully using a gain-scheduled multiobjective controller.

Positive-Position-Feedback (PPF) Control Design

Because the aerodynamics, wing structure, and controller are interconnected dynamic systems, it is possible to control flutter by feeding back an observable state of the system. Of the two measured aeroelastic states, pitch was chosen as a suitable measure of the system because of its high interaction with the air flow and higher coupling with flap deflection.

Positive-position-feedback (PPF) control is used to add damping to the unstable flutter mode. This technique was originally introduced by Goh and Caughey[22] as alternative to collocated-direct-velocity feedback. The control approach consists of feeding back a structural displacement through a second-order filter[23] and is analogous to the tuned-mass vibration damper.

Closed-Loop Results

Models of the plant calculated from system-identification data were used to compute overall damping factors at flow speeds ranging from 10 m/s to 28 m/s. Figure 6 presents plots of the damping factor vs the flow speed for open-loop and closed–loop aeroelastic systems. At speeds greater than 28 m/s, the ambient wind-tunnel noise caused a poor signal-to-noise ratio; thus, identification of the plant did not supply reliable data sets for model computation. Although Fig. 6 presents data up to 28 m/s during the experiment, the system remained stable for flow speeds exceeding 30 m/s. The closed-loop flutter boundary, considered to be 30 m/s, represents an increase by more than 30% over the open-loop flutter boundary.

Figure 7 presents pole migration for open- and closed-loop cases. It can be observed that just as for the open-loop case, the high-frequency pole (pitch) tends to become unstable; however, closed-loop pole frequencies are lower than in the open-loop case for the same flow speed.

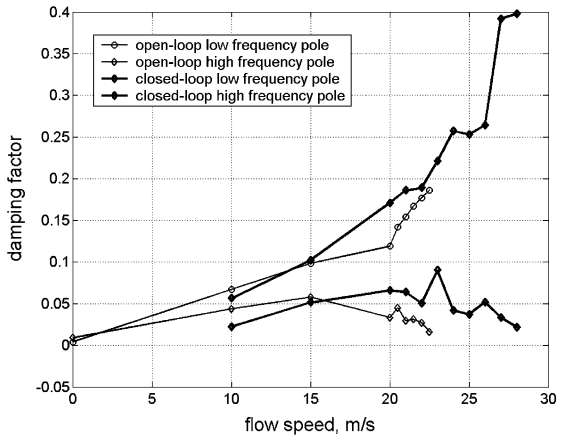

Fig. 6 Variation of damping factor with flow speed in open- and closed-loop designs.

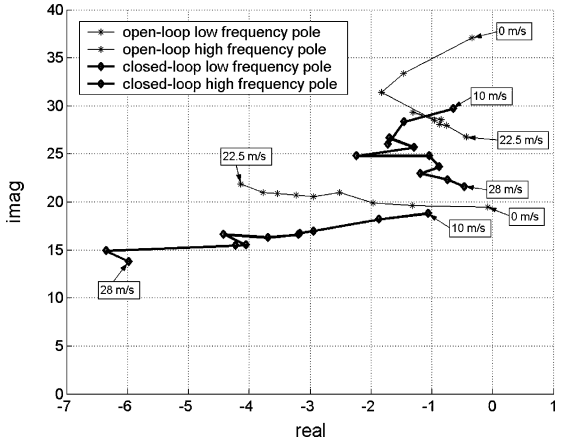

Fig. 7 Pole migration in open- and closed-loop designs.

Conclusions

This work investigated the feasibility of aeroelastic flutter control using trailing-edge control surfaces (flaps) powered by a V-stack piezoelectric actuator. The actuator was integrated into an experimental wing to articulate the trailing-edge flap. The objective was to control the onset of flutter by altering the aerodynamics of the wing by deflecting the trailing-edge flap in a controlled fashion.

By taking advantage of the actuator's shape (V), the actuator was placed chordwise with the output point close to the flap hinge; thus, a simple crank-slider mechanism was used for flap actuation. The mechanism is adjustable and facilitates tuning of the actuator-flap mechanism for desired flap deflection and bandwidth. The actuator produces the desired flap deflection and the response of the flap (angle of deflection), with respect to the voltage applied across the piezoelectric stacks, exhibits the desired linearity, and the actuator-flap system exhibits a bandwidth in excess of 10 Hz.

High control authority and bandwidth facilitated control design. A simple PPF controller was used to add damping to the resonant mode. Operating in closed-loop fashion, the flutter boundary was extended by more than 30%, from 23 to more than 30 m/s. Control authority was remarkable, evidenced by the fact that the unstable wing can be stabilized by closing the loop even while in strong flutter. Reduction of oscillation amplitude was achieved for all flow speeds. Further increase of the flutter speed is deemed possible by using a more sophisticated control approach such as adaptive, Q-parametrization, and gain scheduling approaches. However, this is a topic for future research because the main goal of this work was to investigate the effectiveness of the actuation solution.

Through appropriate changes in design, the flap-actuation solution presented here could be successfully used at smaller or larger scales and for significantly higher flow speeds. For example, in the case of a larger wing, multiple control surfaces, which are individually powered by one V-stack actuator, can be distributed along the trailing edge. One could also conceive of a solution in which multiple actuators power a single control surface and so on. Although this was a demonstration of flutter control of a two-dimensional wing model situated in low aerodynamic pressure, it demonstrated that piezoelectric actuators have the potential for use in real-life applications.

Acknowledgments

This work was supported by Defense Advanced Research Projects Agency through Air Force Office for Scientific Research Grant F49620-99-1-00253, Aeroelastic Leveraging and Control Through Adaptive Structures, under the direction of Ephrahim Garcia and Dan Segalman. We also thank Earl Dowell, Deman Tang, and our colleagues in the Adaptive Systems and Structures Laboratory, David Cox, Robert Richard, Min Moon, and Matthew Kozlowski, for useful discussions and assistance. Thanks to senior machinist John Goodfellow for his effort and commitment in machining the parts.

References

[1]Prechtl, E. F., and Hall, S. R., "Design of High Efficiency, Large Stroke, Electromechanical Actuator," *Smart Materials and Structures*, Vol. 8, 1999, pp. 13–30.

[2]Hall, S. R., and Prechtl, E. F., "Preliminary Testing of a Mach-Scaled Active Rotor Blade with a Trailing Edge Servo-Flap," *Proceedings of the SPIE*, edited by N. M. Wereley, Vol. 3668, 1999, pp. 14–21.

[3]Chandra, R., and Chopra, I., "Actuation of Trailing Edge Flap in a Wing Model Using Piezostack Device," *Journal of Intelligent Material Systems and Structures*, Vol. 9, Oct. 1998, pp. 874–853.

[4]Koratkar, N. A., and Chopra, I., "Analysis and Testing of Mach-Scaled Rotor with Trailing-Edge Flaps," *AIAA Journal*, Vol. 38, No. 7, 2000, pp. 1113–1124.

[5]Borglund, D., and Kuttenkeuler, J., "Active Wing Flutter Suppression Using a Trailing Edge Flap," *Journal of Fluids and Structures*, Vol. 16, No. 3, 2002, pp. 271–294.

[6]Ardelean, E. V., and Clark, R. L., "V-Stack Piezoelectric Actuator," *SPIE Smart Structures and Materials*, Vol. 4333, 2001, pp. 322–333.

[7]Ardelean, E. V., Clark, R. L., and Cole, D. G., "High Performance V-Stack Piezoelectric Actuator," *Journal of Intelligent Material Systems and Structures*, Vol. 15, No. 11, Nov. 2004, pp. 879–889.

[8]Conner, M. D., Tang, D., Dowell, E. H., and Virgin, L. N., "Nonlinear Behavior of a Typical Section Airfoil Section with Control Surface Freeplay: A Numerical and Experimental Study," *Journal of Fluids and Structures*, Vol. 11, No. 1, Jan. 1997, pp. 89–109.

[9]Tang, D., Dowell, E. H., and Virgin, L. N., "Limit Cycle Behavior of an Airfoil with a Control Surface," *Journal of Fluids and Structures*, Vol. 12, No. 7, 1998, pp. 839–858.

[10]Vipperman, J. S., Clark, R. L., Conner, M., and Dowell, E. H., "Experimental Active Control of a Typical Section Using a Trailing-Edge Flap," *Journal of Aircraft*, Vol. 35, No. 2, 1998, pp. 224–229.

[11]Cox, D. E., *Control Design for Parameter-Dependent Aeroelastic Systems*, Ph.D. Dissertation, Dept. of Mechanical Engineering and Materials Science, Duke University, Durham, NC, Aug. 2003.

[12]Karpel, M., "Design for the Active Flutter Suppression and Gust Alleviation Using State-Space Aeroelastic Modeling," *Journal of Aircraft*, Vol. 19, March 1982, pp. 221–227.

[13]Ozbay, H., and Bachmann, G. R., "$\mathcal{H}_2/\mathcal{H}_\infty$ Cotroller Design for Two-Dimensional Thin Airfoil Flutter Suppression," *Journal of Guidance, Control, and Dynamics*, Vol. 17, No. 4, 1994, pp. 722–728.

[14]Ghiringhelli, G. L., Lanz, M., and Mantegazza, P., "Active Flutter Suppression for a Wing Model," *Journal of Aircraft*, Vol. 27, No. 4, 1990, pp. 334–341.

[15]Edwards, J. W., Breakwell, J. V., and Bryson, A. E., "Active Flutter Control Using Unsteady Aerodynamic Theory," *Journal of Guidance and Control*, Vol. 1, No. 1, 1978, pp. 32–40.

[16]Lazarus, K. B., Crawley, E. F., and Lin, C. Y., "Multivariable Active Lifting Surface Control Using Strain Actuation: Analytical and Experimental Results," *Journal of Aircraft*, Vol. 34, No. 3, 1997, pp. 313–321.

[17]Newsom, J. R., "Control Law Synthesis for Active Flutter Suppression Using Optimal Control Theory," *Journal of Guidance and Control*, Vol. 2, No. 5, 1979, pp. 388–394.

[18]Lin, C. Y., and Crawley, E. F., "Design Considerations for a Strain Actuated Adaptive Wing for Aeroelastic Control," *Journal of Intelligent Material Systems and Structures*, Vol. 6, No. 3, 1995, pp. 403–410.

[19]Heeg, J., "Analytical and Experimental Investigation of Flutter Suppression by Piezoelectric Actuation," Technical Paper 3241, NASA, 1993.

[20]Mukhopadhyay, V., "Flutter Suppression Control Law Design and Testing for the Active Flexible Wing," *Journal of Aircraft*, Vol. 32, No. 1, 1995, pp. 45–51.

[21]Waszak, M. R., "Robust Multivariable Flutter Suppression for Benchmark Active Control Technology Wind-Tunnel Model," *Journal of Guidance, Control, and Dynamics*, Vol. 24, No. 1, 2001, pp. 147–153.

[22]Goh, C. J., and Caughey, T. K., "On the Stability Problem Caused by Finite Actuator Dynamics in the Control of Large Space Structures," *International Journal of Control*, Vol. 41, No. 3, 1985, pp. 787–802.

[23]Fanson, J., and Caughey, T., "Positive Position Feedback Control for Large Space Structures," *AIAA Journal*, Vol. 28, No. 4, 1990, pp. 717–724.